Combination of chloroquine diphosphate and salidroside induces human liver cell apoptosis via regulation of mitochondrial dysfunction and autophagy

BING JIANG[1], LONGFEI FENG[1], TAO YANG[1], WENJING GUO[1], YANGYANG LI[1], TAO WANG[2], CHENGGUANG LIU[3] and HAIXIANG SU[1,2]

[1]School of Basic Medicine, Gansu University of Traditional Chinese Medicine, Lanzhou, Gansu 730000; [2]Translational Medicine Research Center, Gansu Provincial Academic Institute for Medical Research, Gansu Provincial Cancer Hospital, Lanzhou, Gansu 730050; [3]Clinical College of Integrated Chinese and Western Medicine, Guangxi University of Traditional Chinese Medicine, Nanning, Guangxi 530200, P.R. China

Received August 22, 2022; Accepted November 24, 2022

DOI: 10.3892/mmr.2022.12924

Abstract. Hepatocellular carcinoma (HCC) is the leading cause of cancer-associated death in the world. Chemotherapy remains the primary treatment method for HCC. Despite advances in chemotherapy and modalities, recurrence and resistance limit therapeutic success. Salidroside (Sal), a bioactive component extracted from the rhizome of *Rhodiola rosea* L, exhibits a spectrum of biological activities including antitumor effects. In the present study, it was demonstrated that Sal could induce apoptosis and autophagy of 97H cells by using CCK-8 assay, transmission electron microscopy (TEM), Hoechst33342 staining, MDC staining, western blotting. Pretreatment with Sal enhanced apoptosis and autophagy via upregulation of expression levels of Bax, Caspase-3, Caspase-9, light chain (LC)3-II and Beclin-1 proteins and downregulation of expression levels of Bcl-2, LC3-I and p62 protein in 97H cells. Furthermore, Sal was demonstrated to inhibit activation of the PI3K/Akt/mTOR signaling pathway and, when combined with autophagy inhibitor chloroquine diphosphate (CQ), increased phosphorylation of PI3K, Akt and mTOR proteins. The combined treatment with Sal and CQ not only decreased Sal-induced autophagy, but also accelerated Sal-induced apoptosis. Therefore, Sal-induced autophagy might serve a role as a defense mechanism in human liver cancer cells and its inhibition may be a promising strategy for the adjuvant chemotherapy of liver cancer.

Correspondence to: Professor Haixiang Su, Translational Medicine Research Center, Gansu Provincial Academic Institute for Medical Research, Gansu Provincial Cancer Hospital, 2 Xiaoxihu East Street, Qilihe, Lanzhou, Gansu 730050, P.R. China
E-mail: shxsuhaixiang54120@163.com

Key words: salidroside, chloroquine diphosphate, liver cancer, apoptosis, autophagy, PI3K/Akt/mTOR

Introduction

Hepatocellular carcinoma (HCC) was the sixth most commonly reported cancer and the third most common cause of cancer death in the world in 2020 (1). With research of HCC, the methods of treatment have developed rapidly. Following traditional surgery, radiotherapy and chemotherapy, novel methods (such as interventional, molecular targeted and cell therapy and immunotherapy) have been widely used in the treatment of HCC (2-4). However, the prognosis of most patients is still poor, which is related to the poor response of regimens for treatment (5), numerous side effects (including gastrointestinal reaction, cutaneous pruritus) (6) and multidrug resistance (7). Therefore, exploration of effective and safe drugs for the treatment of HCC is an urgent clinical problem.

Rhodiola rosea L, also known as 'golden root', is a perennial herbaceous plant of the crassulaceae family and is widely distributed in zones with severe cold, dry and hypoxic conditions at high altitude (3,500-5,000 meters) (8). In Asia, *Rhodiola rosea* L is used as a herbal medicine to relieve certain symptoms, such as headache and hernias (9). In Europe and North America, *Rhodiola rosea* L is used as a dietary supplement (10,11). According to modern pharmacology reports, the key metabolites of *Rhodiola rosea* L include phenethyl alcohol derivatives, monoterpenes, triterpenes, flavonoids and phenolic acids (12,13). Salidroside (Sal), a primary component, is extracted from the rhizome of *Rhodiola rosea* L. An increasing number of studies have reported that Sal not only demonstrates anti-hypoxia and anti-aging effects (14,15), but also demonstrates anti-fibrotic and immune regulatory effects (16,17). Therefore, development of Sal for treatment of disease is a promising field.

Induction of cancer cell apoptosis is one of the goals of anti-cancer treatment. Apoptosis is an active physiological response and the primary form of type I programmed cell death, which is characterized by eversion of the membrane, condensation of nuclear chromatin, splitting of the nucleus and formation of apoptotic bodies (18). Autophagy is a pathway of type II programmed cell death, which is different from

apoptosis. Autophagy primarily refers to the action of autophagic vesicles, which wrap senescent or damaged organelles in a double-layered membrane to form autophagosomes when cells receive certain stimuli (such as starvation or hypoxia). Autophagosomes combine with lysosomes to form autolysosomes, which degrade the wrapped contents to maintain the stability of internal environment and the renewal of organelles (19). Autophagy has become a hot topic in anti-cancer therapy (20,21). At present, the association between autophagy and apoptosis is still controversial (22). In tumorigenesis and development, autophagy may serve two opposite roles; autophagy can act as a protective mechanism to resist stress response and inhibit apoptosis. For example, Wang *et al* (23) reported that pseudolaric acid B induces autophagy and inhibits apoptosis in human lung fibroblast MRC5 cells via the response to DNA damage. Furthermore, autophagy produces certain products (such as amino acids and fatty acids), which provide nutrients for the growth of tumor (24,25). However, autophagy synergistically induces apoptosis. For example, resveratrol synergistically treats ovarian cancer by inducing autophagy in human ovarian cancer cells (26). Combined treatment with matrine and 5-fluorouracil upregulates expression of autophagy-associated genes Atg5 and Beclin-1 to enhance the chemosensitivity of liver cancer cells (27). Thus, autophagy exerts a dual effect in the therapy of cancer.

Increasing studies have reported that glycosides, which are derived from traditional Chinese medicine, treat cancer through the autophagy pathway (28,29). For example, ginsenoside F2 induces autophagy by upregulating expression levels of Atg7, Beclin-1 and microtubule-associated protein light chain 3 (LC3)B proteins in human breast cancer stem cells; moreover, combined treatment with the autophagy inhibitor chloroquine enhances ginsenoside F2-induced apoptosis (30). Pulsatilla saponin D induces autophagy by activating phosphorylation of ERK and inhibiting phosphorylation of mTOR and p70S6K, which enhances the level of human cervical cancer HeLa cell apoptosis (31).

There are numerous reports for the use of Sal in the treatment of cancer (32,33), but to the best of our knowledge, there are few studies (34,35) on Sal-induced apoptosis and autophagy of liver cancer cells in Chinese and international literature. In particular, there are no reports on the mechanism of Sal-induced apoptosis and autophagy in liver cancer cells. Therefore, in the present study, the mechanisms of Sal-induced apoptosis and autophagy in highly metastatic human hepatoma cells (MHCC97-H, 97H) were evaluated. Moreover, to assess the association between autophagy and apoptosis, chloroquine diphosphate (CQ), a commonly used inhibitor of the autophagic pathway, was used in the present study.

Materials and methods

Reagents and antibodies. Sal (purity, 99.56%), CQ (purity, 99.65%) and rapamycin (Rap; purity, 99.30%) were purchased from Selleck Chemicals. DMEM, RPMI-1640 medium and phosphate-buffered saline (PBS) were purchased from Cytiva. Trypsin-EDTA solution, 1% crystal violet stain solution, 1% osmium tetroxide, saturated uranyl acetate, lead citrate, Hoechst33342 dye, dansylcadaverine (MDC, cat. no. G0170) staining kit, radioimmunoprecipitation assay (RIPA, cat. no. R0010), phenylmethylsulfonyl fluoride (PMSF, cat. no. P0100), SDS-PAGE gel preparation kit (cat. no. P1200), Tween-20, 10% SDS, 20X Tris-HCl buffered saline, 10X transfer buffer, BCA protein assay kit and 4X bromophenol blue buffer were purchased from Beijing Solarbio Science & Technology Co., Ltd.

Penicillin-streptomycin (100X) was purchased from Shanghai Basal Media Technologies Co., Ltd. Fetal bovine serum (FBS) was purchased from Sartorius AG. 4.0 and 2.5% paraformaldehyde and extra-enhanced chemiluminescence substrate kit (cat. no. BL520A) were purchased from Biosharp Life Sciences. Cell Counting Kit-8 (CCK-8) and three-color pre-stained protein marker were purchased from Yeasen Biotechnology (Shanghai) Co., Ltd. 95% absolute ethanol was purchased from Tianjin Damao Chemical Reagent Factory Difco™ skimmed milk and glycine were purchased from Beijing Biotopped Technology Co., Ltd. Tris was purchased from Shanghai Scigrace Biotech Co., Ltd. Anti-β-actin (cat. no. GTX109639), anti-GAPDH (cat. no. GTX627408), anti-β-tubulin (cat. no. GTX101279) and anti-p62 (cat. no. GTX100685) antibodies were purchased from GeneTex, Inc. Anti-C-myc (cat. no. 67447-1-Ig), anti-Bax (cat. no. 60267-1-Ig), anti-Bcl-2 (cat. no. 12789-1-AP), anti-Caspase-3 (cat. no. 19677-1-AP), anti-Caspase-9 (cat. no. 10380-1-AP) and anti-Beclin-1 (cat. no. 1C10C4) antibodies were purchased from ProteinTech Group, Inc. Anti-LC3-I/II (cat. no. ab192890) antibodies were purchased from Abcam. Anti-PI3K (cat. no. YM3503), anti-p-PI3K (cat. no. YP0765), anti-Akt (cat. no. YT0185), anti-p-Akt (cat. no. YP0006), anti-mTOR (YT2913) and anti-p-mTOR (YP0176) antibodies were purchased from ImmunoWay Biotechnology Company. Horseradish peroxidase-conjugated goat anti-rabbit IgG antibodies (cat. no. TA130023) were purchased from OriGene Technologies, Inc.

Cell culture and treatment. The hepatocellular carcinoma 97H and epithelial THLE-2 and Hs578Bst cell lines were purchased from the Cell Bank of The Shanghai Institute for Biological Sciences. 97H cells were cultured in DMEM with 10% FBS. THLE-2 and Hs578Bst cells were cultured in RPMI-1640 medium with 10% FBS. All cells were incubated at 37˚C in a humidified atmosphere with 5% CO_2. Cells were treated with or without Sal (5, 10, 20, 40 and 80 μM) and/or CQ (5, 10 and 20 μM) for 24, 48 and 72 h at 37˚C. Cells were also treated with or without Sal (80 μM) and/or Rap (400 nM) for 48 h at 37˚C.

Cell growth curve. The 97H cells (80-90% confluence) were seeded in 12-well plates (3,000 cells/well) at 37˚C for 24 h. Following incubation, the number of untreated 97H cells was assessed using a multifunctional cell analyzer (ACEABioscience, Inc.).

Cell viability assay. 97H, THLE-2 and Hs578Bst cells ($5x10^3$ cells/well) were seeded in 96-well plates and incubated at 37˚C with 5% CO_2 in a humidified environment for 24 h. The cells were treated with Sal (0, 5, 10, 20, 40 and 80 μM) and/or CQ (5, 10 and 20 μM), as aforementioned. A total of 10 μl CCK-8 reagent was added into each well and the cells were incubated at 37˚C in the dark for 1 h. The cell viability

assay was performed using a microplate reader (Bio-Rad Laboratories, Inc.; excitation wavelength, 450 nm).

Colony formation assay. 97H cells (80-90% confluence) were seeded in 60-mm dishes (500 cells/ml) and incubated at 37˚C for 24 h. Following incubation, the untreated cells in the blank group and treated 97H cells were washed twice using PBS, cultured with complete medium (10% FBS + 90% DMEM) and incubated in the incubator (5% CO_2, 37˚C) for 14 days. The colonies (>50 cells) were fixed using 4% paraformaldehyde for 30 min at room temperature and stained using 1% crystal violet for 30 min at room temperature. Stained cells were observed and photographed using an inverted microscope (Olympus Corporation, magnification, x40, x200), and the colonies of each group were counted manually.

Transmission electron microscopy (TEM). To evaluate the ultrastructure, cells in the blank group and treated 97H cells were washed twice with PBS. Cells were fixed using 2.5% paraformaldehyde for 90 min and 1% osmium tetroxide for 30 min at 37˚C. Following gradient dehydration with 95% absolute ethanol, cells were embedded in the resin, sectioned into 60 nm thin slices, stained using saturated uranyl acetate for 30 min at 37˚C, and stained using lead citrate for 10 min at 37˚C. Images were captured using a transmission electron microscope (Hitachi, Ltd.; magnification, x5,000 and x8,000).

Hoechst33342 staining. 97H cells (80-90% confluence) were incubated on a glass slide in 12-well plates at 37˚C for 24 h. Following incubation, the glass slides were washed twice with PBS and cells were fixed using 4% paraformaldehyde for 30 min at 37˚C. Glass slides were stained using 10 μg/ml Hoechst33342 dye for 30 min in the dark at 37˚C and washed twice with PBS. Stained cells were observed using a fluorescence microscope (Olympus Corporation; excitation wavelength, 488 nm; magnification, x100 and x200).

MDC staining. 97H cells (80-90% confluence) were plated on glass slides in 12-well plates at 37˚C for 24 h. Following incubation, cells in blank group and treated 97H cells were washed twice with 1X wash buffer, stained with MDC dye for 30 min in the dark at 37˚C and washed again with 1X wash buffer three times. Stained cells were observed under a fluorescence microscope (excitation wavelength, 355 nm; magnification, x200).

Western blotting. Cells in the blank group and treated 97H cells were lysed using pre-cooled RIPA lysis buffer (500 μl RIPA; 5 μl PMSF) for 30 min at 4˚C. Protein concentration was assessed using BCA protein assay kit. Protein (30 μg/lane) was separated using 6, 10 and 15% SDS-PAGE. According to the different molecular weight of the target protein, the corresponding concentration of SDS-PAGE was selected. Subsequently, the SDS-PAGE was transferred to polyvinylidene fluoride membranes. Membranes were blocked using 5% skimmed milk for 2 h at room temperature and washed using Tris-buffered saline with 0.1% Tween-20 for 15 min at room temperature. Membranes were probed at 4˚C overnight with antibodies as follows: Anti-β-actin (1:2,000), anti-GAPDH (1:5,000), anti-β-tubulin (1:2,000), anti-C-myc (1:1,000), anti-Bax (1:1,000), anti-Bcl-2 (1:1,000), anti-Caspase-3 (1:1,000), anti-caspase-9 (1:1,000), anti-Beclin-1 (1:2,000), anti-p62 (1:1,000), anti-LC3-I/II (1:1,000), anti-PI3K (1:1,000), anti-p-PI3K (1:500), anti-Akt (1:1,000), anti-p-Akt (1:1,000), anti-mTOR (1:1,000) and anti-p-mTOR (1:500). Membranes were incubated with horseradish peroxidase-conjugated goat anti-rabbit IgG antibody (1:5,000) for 2 h at room temperature. Protein expression was assessed using an extra-enhanced chemiluminescence substrate kit and gel imaging system (Bio-Rad Laboratories, Inc.). Protein expression levels were semi-quantified using Image Lab 5.1.0 software (Bio-Rad Laboratories, Inc.) and processed using GraphPad Prism 8.0.2 software (GraphPad Software, Inc.).

Statistical analysis. All experiments were performed at least three times. The data are presented as the mean ± standard deviation. Statistical analysis was performed using SPSS 22.0 statistical software (IBM Corp.). Differences between multiple groups were compared using one-way ANOVA followed by Tukey's post hoc test. $P<0.05$ was considered to indicate a statistically significant difference.

Results

Sal suppresses proliferation of 97H cells in vitro. The growth curves of 97H cells were assessed using a multifunctional cell analyzer without any drug intervention. The growth curve of untreated cells can be divided into slow growth latency (0-25 h), exponential growth phase with a larger slope (25-70 h), plateau-shaped flat-top phase (70-90 h) and degenerate decay phase (90-95 h) (Fig. 1A). These data provided a basis for the processing time of subsequent experiments. 97H cells were treated with Sal (5, 10, 20, 40 and 80 μM) for 24, 48 and 72 h. Compared with the blank group, Sal demonstrated significant inhibitory effects on viability of 97H cells in a dose-dependent manner at different times ($P<0.01$; Fig. 1B). The values of half maximal inhibitory concentration (IC_{50}) at 24, 48 and 72 h were 119.2, 29.1 and 14.1 μM respectively (Fig. 1C). To evaluate the safety of Sal, normal human liver THLE-2 cells and normal human breast Hs578Bst cells were treated with Sal (5, 10, 20, 40 and 80 μM) for 48 h. Sal had no significant effect on the viability of THLE-2 and Hs578Bst cells ($P>0.05$; Fig. 1D). Based on these results, it was decided to treat 97H cells with 20, 40 and 80 μM Sal for 48 h in subsequent experiments. Following treatment with Sal (20, 40 and 80 μM) for 48 h, compared with the blank group, the Sal group markedly decreased the number of 97H colonies in a dose-dependent manner (Fig. 1E). Results of western blotting demonstrated that compared with the blank group, expression levels of C-myc protein in the Sal group were significantly down-regulated in a dose-dependent manner ($P<0.05$; Fig. 1F).

Sal induces organelle impairment and autophagy. In the present study, TEM was used to evaluate the organelle of 97H cells following Sal or autophagic inducer (Rap) treatment. The mitochondria of blank cells were rich in content, uniform in size, clear in mitochondrial crista, and complete in membranous structure (Fig. 2A), numerous damaged mitochondria were observed in the Sal- or Rap-treated 97H cells at 48 h (Fig. 2B and C, respectively). Furthermore, numerous

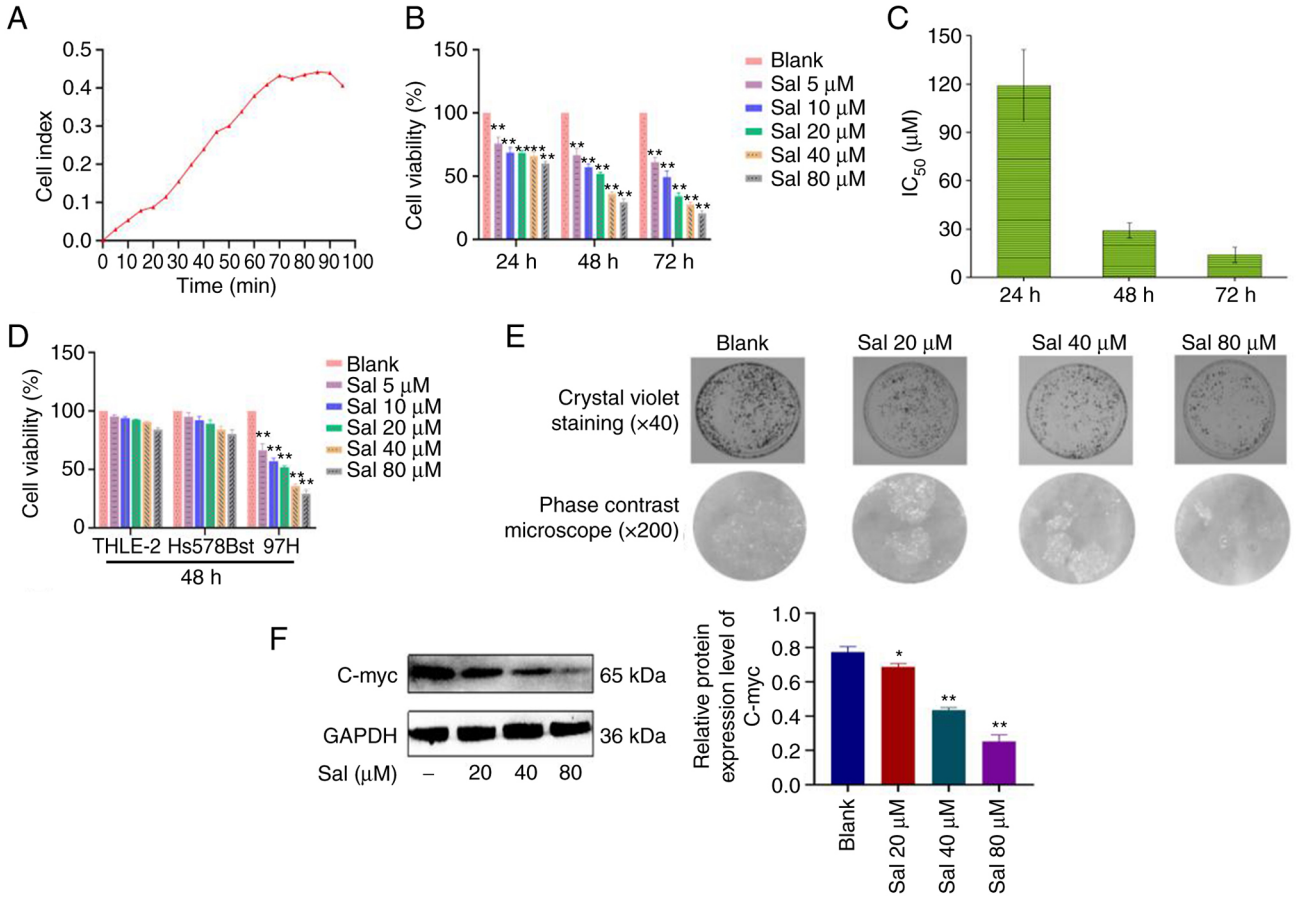

Figure 1. Sal suppresses viability in 97H cells. (A) Natural growth curve of 97H cells. (B) Effects of Sal on the viability of 97H cells assessed using Cell Counting Kit-8 method. (C) IC_{50} for Sal in Sal-treated 97H cells. (D) Effects of Sal on THLE-2 and Hs578Bst cell viability. (E) Effects of Sal on the self-renewal ability of 97H cells was assessed using plate colony formation experiment. Magnification, x40, x200. (F) Expression levels of C-myc protein were semi-quantified using western blotting in 97H cells. *P<0.05 and **P<0.01 vs. blank. Sal, salidroside; IC_{50}, half maximal inhibitory concentration.

autophagosomes with double membranes were observed in the Sal or Rap-treated 97H cells at 48 h. Cytoplasmic material and/or membrane vesicles were encapsulated within the autophagosomes. To evaluate the phenomenon of autophagy, MDC staining was used to assess the autophagy product (autophagosomes) following Sal or Rap treatment in 97H cells. The green fluorescence associated with autophagosomes was not demonstrated in the blank group; green fluorescence was gradually increased in a dose-dependent manner in the Sal or Rap-treated 97H cells (Fig. 2D). Western blotting demonstrated that compared with the blank and Rap group, the ratio of LC3-II to LC3-I protein expression levels was markedly upregulated in the Sal group with a dose-dependent manner (P<0.05); meanwhile, the Beclin-1 protein expression levels in the Sal group were significantly upregulated in a dose-dependent manner (P<0.05); furthermore, expression levels of p62 protein in the Sal group were significantly downregulated in a dose-dependent manner (P<0.05; Fig. 2E).

These results indicated that Sal or Rap treatment resulted in organelle impairment and induced autophagy.

Sal induces apoptosis in 97H cells. Hoechst33342 staining demonstrated markedly increased numbers of apoptotic cells in a dose-dependent manner in Sal-treated groups (Fig. 3A). To evaluate the apoptotic effect induced by Sal, expression levels of mitochondrial apoptosis-related proteins were assessed using western blotting (Fig. 3B). The results demonstrated that compared with the blank group, the ratio of the Bcl-2 to Bax protein expression levels was significantly down-regulated. Furthermore, expression levels of Caspase-3 and Caspase-9 proteins were significantly up-regulated in a dose-dependent manner at 48 h after treatment with Sal (P<0.01). These results suggested that Sal could induce 97H cells apoptosis.

Inhibiting autophagy increases mitochondrial damage in 97H cells. CQ is commonly used as an autophagy inhibitor. It has been reported to inhibit autophagy by preventing the combination of autophagosomes and lysosomes (36). Therefore, in the present study, CQ was used to inhibit autophagy. Compared with the blank and Sal groups, the amount and brightness of green fluorescence was markedly decreased in a dose-dependent manner in the Sal + CQ group (Fig. 4A). Furthermore, p62 protein expression levels were significantly upregulated and Beclin-1 and LC3-II/I protein expression levels were significantly downregulated following treatment with CQ compared with the Sal group (P<0.01; Fig. 4B). Moreover, Beclin-1 protein expression levels were significantly upregulated and p62 protein expression levels were significantly downregulated following treatment with

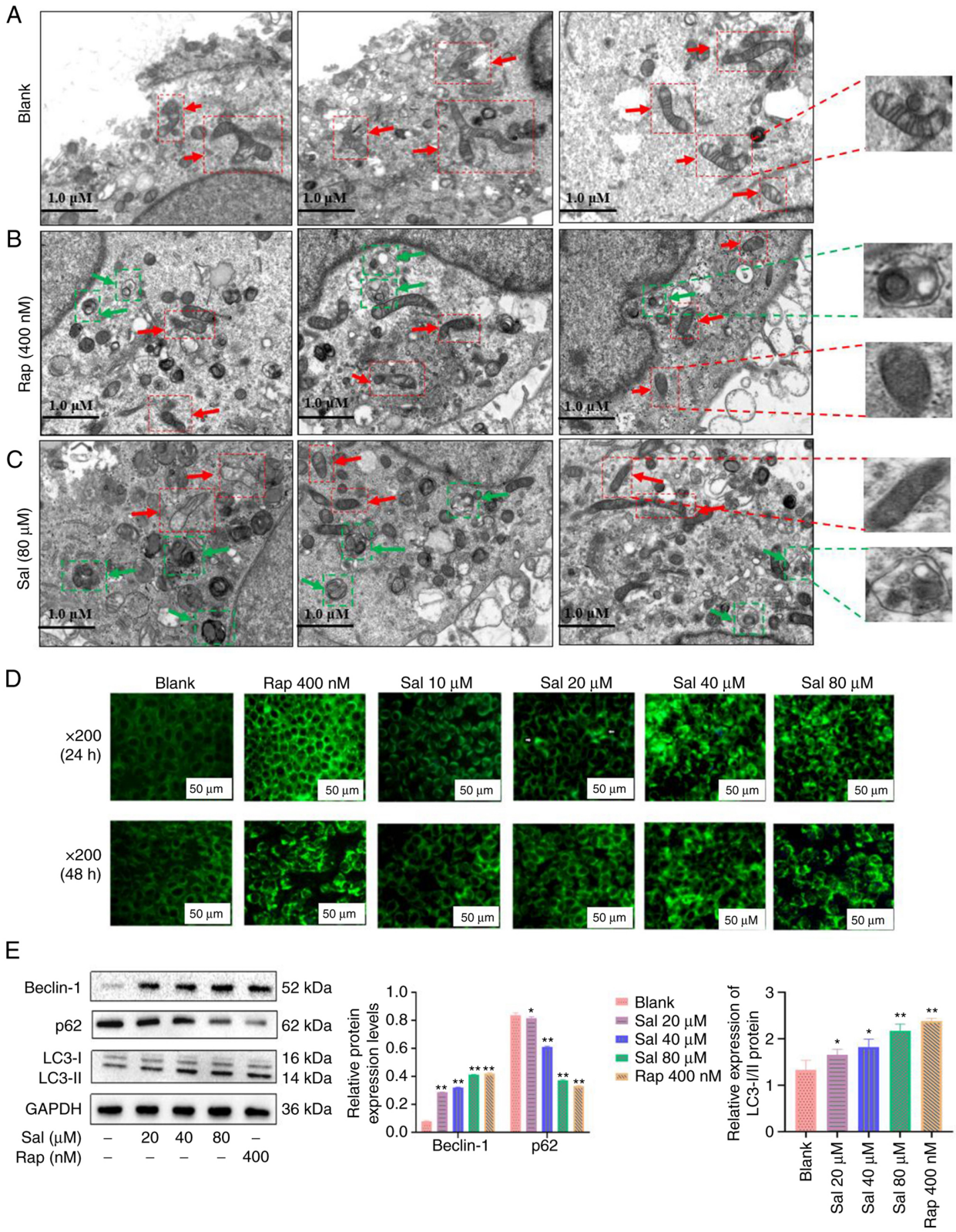

Figure 2. Sal induces autophagy in 97H cells. (A) Untreated 97H cells were assessed using TEM. The mitochondria of the blank group were normal. Swollen mitochondria and autophagosomes in the cytoplasm were observed in (B) Rap and (C) Sal treatment groups. Red arrowheads indicate mitochondria and green arrowheads indicate autophagosomes. (D) Green fluorescence associated with autophagosomes was markedly increased in a dose-dependent manner using MDC staining in the Sal and Rap treatment groups, compared with the blank group. Magnification, x200. (E) Expression levels of Beclin-1, p62, LC3-I and LC3-II proteins were semi-quantified using western blotting in 97H cells. *P<0.05 and **P<0.01 vs. blank. Sal, salidroside; Rap, rapamycin.

the autophagy inducer Rap compared with the Sal group (P<0.01; Fig. 4C). These data indicated that CQ effectively inhibited Sal-induced autophagy in the present study.

Mitochondria are not only key organelles for the production of energy, but also regulate cellular redox signaling pathways and programmed cell death (37). To evaluate the

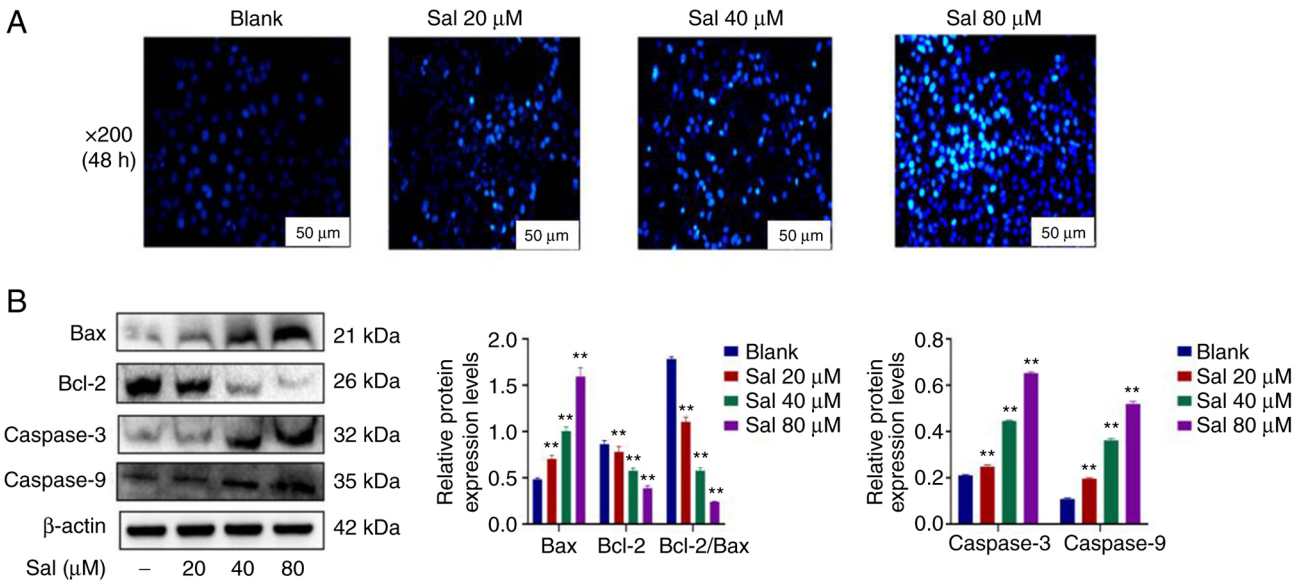

Figure 3. Sal induces apoptosis in 97H cells. (A) Apoptosis was assessed using Hoechst33342 staining in 97H cells. Compared with the blank group, the number of apoptotic cells was markedly increased in a dose-dependent manner in the Sal treatment groups. Magnification, x200. (B) Protein expression levels of Bax, Bcl-2, Caspase-3 and Caspase-9 were semi-quantified using western blotting in 97H cells. **P<0.01 vs. blank. Sal, salidroside.

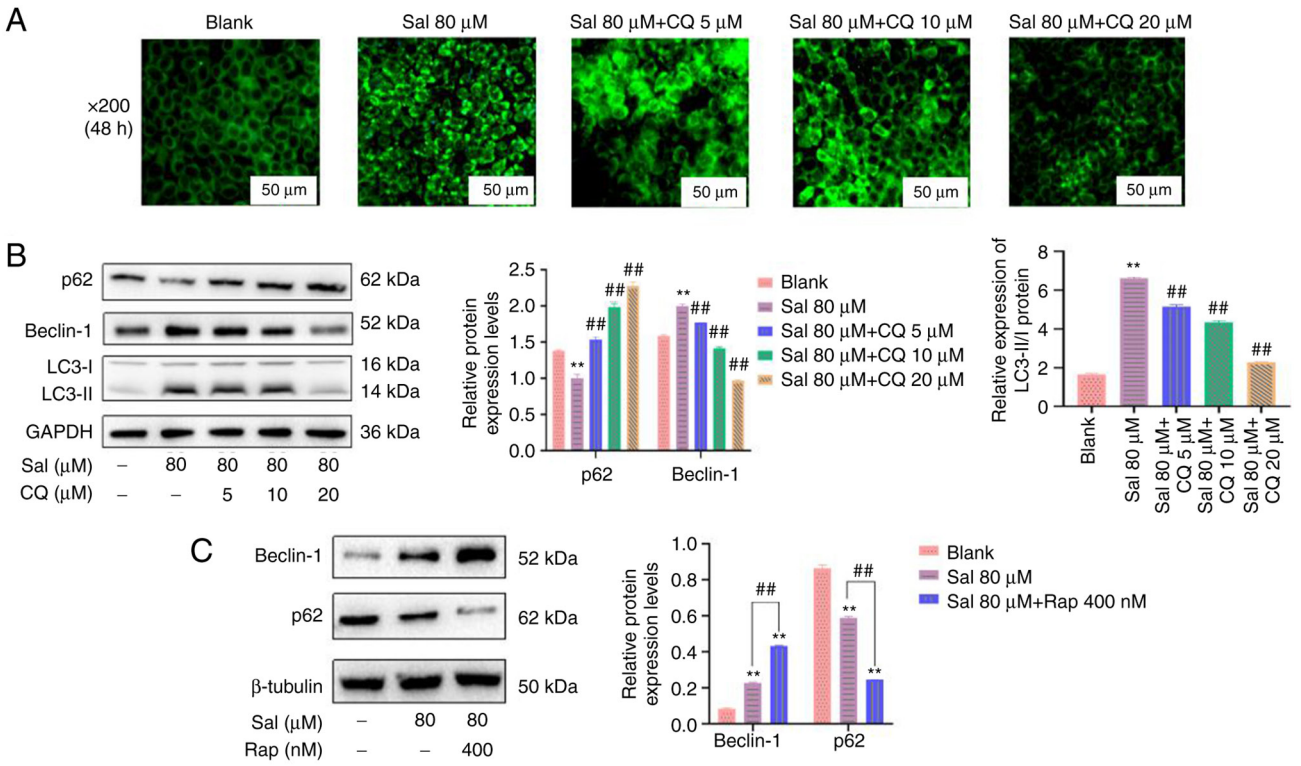

Figure 4. CQ inhibits Sal-induced autophagy in 97H cells. (A) Green fluorescence associated with autophagosomes was decreased in a dose-dependent manner using MDC staining in the Sal + CQ treatment group compared with blank and Sal groups. Magnification, x200. (B) Expression levels of p62, Beclin-1, LC3-I and LC3-II proteins were semi-quantified using western blotting in 97H cells treated with Sal and/or CQ. (C) Protein expression of Beclin-1 and p62 was semi-quantified using western blotting in 97H cells treated with Sal and/or Rap. **P<0.01 vs. blank. $^{\#\#}$P<0.01 vs. Sal. CQ, chloroquine diphosphate; Sal, salidroside; Rap, rapamycin.

effect of CQ on Sal-treated mitochondria, TEM was used to assess the ultrastructure of mitochondria (Fig. 5A-C). Swollen mitochondria were demonstrated following Sal treatment, compared with the blank group. Furthermore, more serious mitochondrial damage was observed in the Sal + CQ group (Fig. 5C), including swollen mitochondria, double-membrane destruction and loss of normal morphology. These results demonstrated that inhibiting autophagy increased the extent of mitochondrial damage in Sal-treated cells.

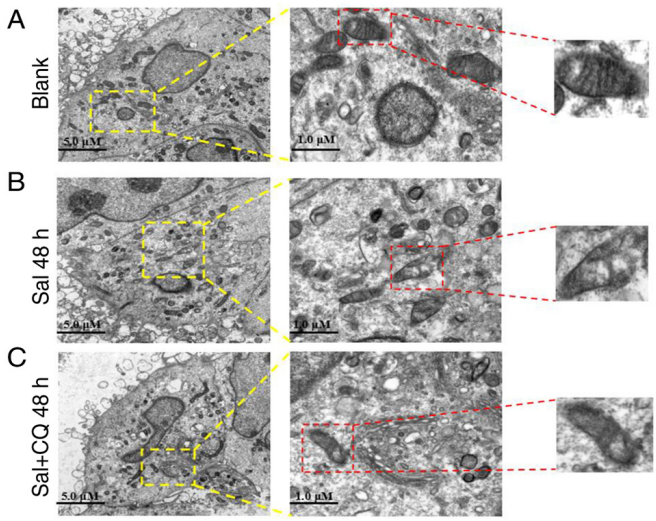

Figure 5. Inhibition of autophagy increases mitochondrial impairment in 97H cells. The ultrastructure of mitochondria in each group was assessed. (A) Mitochondrial morphology was normal in the blank group. (B) Swollen mitochondria were observed following Sal treatment for 48 h in 97H cells. (C) Cells were treated with Sal and CQ for 48 h. Compared with the blank and Sal groups, increased damage to mitochondrial morphology was observed. CQ, chloroquine diphosphate; Sal, salidroside.

Taken together, these results suggested that inhibition of autophagy increased the degree of mitochondrial damage.

Inhibiting autophagy enhances Sal-induced apoptosis. To evaluate the apoptotic effect of CQ in Sal-treated 97H cells, CCK-8 method, plate colony formation assay and Hochest33342 staining were used to assess apoptosis. The results demonstrated that compared with the blank group, 80 μM Sal group both demonstrated inhibitory effects on viability of 97H cells at different times (P<0.01). Moreover, compared with the Sal group, the viability of 97H cells was all decreased significantly with a dose-dependent manner in the Sal + CQ groups at different times (P<0.01; Fig. 6A). As seen in Fig. 6B, compared with the blank group, the number of 97H cells' colonies was decreased at 48 h after treatment with 80 μM Sal, and fewer colonies appeared in the Sal + CQ groups at 48 h after treatment. The result of Hoechst33342 staining demonstrated the number of apoptotic cells was markedly increased at 48 h after treatment with Sal. More apoptotic cells were demonstrated in the Sal + CQ groups at 48 h after treatment compared with the blank (Fig. 6C).

Taken together, these results suggested that inhibition of autophagy increased apoptosis.

CQ regulates expression of Caspases in 97H cells. The caspase family serves an important role in mitochondrially-regulated programmed death (38). Following Sal treatment, Caspase-3, Caspase-9 and Bax/Bcl-2 protein expression levels all demonstrated significant increases compared with the blank (P<0.01; Fig. 7A and B). Following combination with CQ treatment, compared with the blank and Sal groups, protein expression levels of Caspase-3, Caspase-9, Bax and Bcl-2 were significantly increased (P<0.01). These results indicated that inhibition of autophagy increased apoptosis and this may be associated with the Caspase-mediated intrinsic apoptosis pathway in 97H cells.

Sal and CQ regulate the PI3K/Akt/mTOR signaling pathway. Western blotting demonstrated that compared with the blank group, the ratios of p-PI3K/PI3K, p-Akt/Akt and p-mTOR/mTOR proteins were significantly decreased with a dose-dependent manner in the Sal group (P<0.01; Fig. 8A and B). Compared with the Sal group, combined treatment with Sal and CQ promoted the ratios of p-PI3K/PI3K, p-Akt/Akt and p-mTOR/mTOR proteins in a dose-dependent manner (P<0.01; Fig. 8C and D). These data demonstrated that Sal induced autophagy via inhibition of the activation of the PI3K/Akt/mTOR signaling pathway. Inhibition of autophagy may have increased apoptosis via the PI3K/Akt/mTOR signaling pathway in 97H cells.

Discussion

In the present study, a Sal-treated 97H cell model *in vitro* demonstrated that both apoptosis and autophagy were increased following treatment with Sal. Further experiments demonstrated that combination treatment with CQ and Sal inhibited autophagy and promoted apoptosis, which indicated that inhibitors of autophagy might accelerate the apoptotic process of 97H cells. The results of the present study may aid in the elucidation of the underlying molecular mechanisms of crosstalk between autophagy and apoptosis in the stress-stimulated environment, which may contribute to the development of novel therapy for liver cancer. In cell biology, autophagy defines the catabolic process that regulates the degradation of cell components through the lysosomal machinery (39). Apoptosis is a process of programmed cell death in normal physiological conditions and is also an important part of maintaining the homeostasis of internal environment (40). As two distinct self-destructive processes, apoptosis ('self-killing') and autophagy ('self-eating') are initiated and regulated by their own molecular mechanism (40). However, a complex relationship exists between autophagy and the apoptotic cell death pathway, whereby regulators of apoptosis also serve as regulators of autophagic activation (41).

Inhibition of autophagy by using specific inhibitors (such as CQ) or suppression of autophagy regulatory pathways, may increase the apoptotic efficiency of chemotherapeutic agents in pancreatic (42), breast (43), colon (44) and lung cancer (45) cells. These reports indicated that autophagy may also be a therapeutic approach for cancer and that inhibition of autophagy significantly promotes occurrence of apoptosis in the development of cancer. Moreover, reports indicate that CQ and interventional therapy combination may exert a synergistic effect and induce apoptosis in Wistar liver cancer rats (46,47). Similar to these results, in the present study, Sal induced apoptosis and autophagy in the human 97H liver cancer cell line. The viability of 97H cells incubated in Sal-treated culture was evaluated. The viability of 97H cells after Sal treatment was markedly lower compared with that of normally cultured cells assessed using CCK-8 assay, Hoechst33342 staining and western blotting. Cells were more dispersed and decreased in number in the Sal + CQ group. Autophagosomes are key elements in autophagy (48). Many methods can be used to

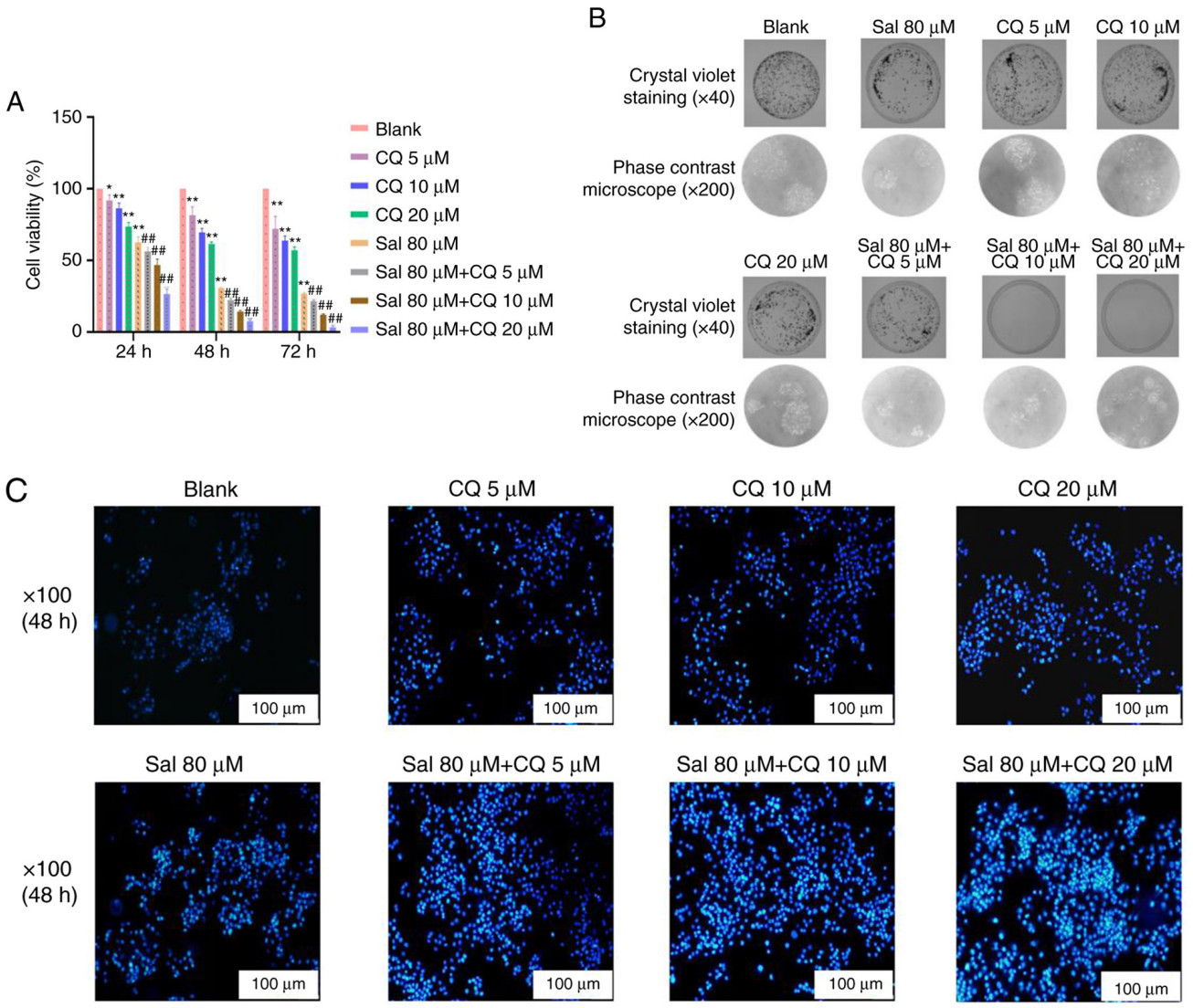

Figure 6. Inhibition of autophagy enhances Sal-induced apoptosis in 97H cells. (A) Effects of Sal combined with CQ on viability of 97H cells were assessed using Cell Counting Kit-8. (B) Effects of Sal combined with CQ on self-renewal ability of 97H cells was evaluated using the plate colony formation experiment. Magnification, x40, x200. (C) Apoptosis was assessed using Hoechst33342 staining in 97H cells. Compared with the blank and San group, the number of apoptotic cells was markedly increased in a dose-dependent manner in the Sal + CQ group. Magnification, x100. *P<0.05 and **P<0.01 vs. blank. $^{\#\#}$P<0.01 vs. Sal. CQ, chloroquine diphosphate; Sal, salidroside.

detected the formation of autophagosomes. For example, Zhang *et al* (49) observed changes of autophagosomes in hypoxia-induce myocardial cells injury in mice using TEM technique. Cui *et al* (50) used MDC staining to detect the number of autophagosomes in each group to evaluate the effect of hydroxysafflor yellow A on the formation of autophagosomes in vascular adventitial fibroblasts (VAFs) induced by angiotensinogen II. Similar to their results, we also observed the formation of autophagosomes in 97H cells treated with Sal or Rap by using the TEM and MDC staining. Beclin-1, p62 and LC3B have been reported to be key proteins in autophagy. The Beclin-1 gene, which encodes the autophagy-induced protein, has been reported to regulate localization of other autophagy proteins in the structure of autophagy precursors by forming a complex with type III PI3K, which regulates autophagy activity (51,52). p62 protein is reported to bind LC3 in the membrane of the autophagic vesicle to recruit the autophagic degradation substrate into the autophagic vesicle for degradation (53,54). LC3 is a soluble, cytosolic protein that is cleaved during autophagic induction and is involved in the formation of the autophagic vacuole membrane. When the autophagic process starts, LC3-I (16 kDa) is converted to LC3-II (14 kDa) (55,56). Therefore, western blotting was used to assess protein expression levels of Beclin-1, p62, LC3-II and LC3-I in Sal-treated 97H cells to evaluate the level of cell autophagy. Following Sal treatment, the number of autophagosomes gradually increased, Beclin-1 protein expression levels and LC3-II/LC3-I ratio also increased, whereas p62 protein expression levels decreased, which indicated that Sal increased cell autophagy.

In the present study, Sal induced apoptosis and autophagy in 97H cells. Based on these findings and related literature (57,58), it could be hypothesized that Sal-induced autophagy is a protective mechanism for hepatoma cells and that inhibition of autophagy may promote apoptosis. To evaluate this hypothesis, autophagy agonists were used as positive controls

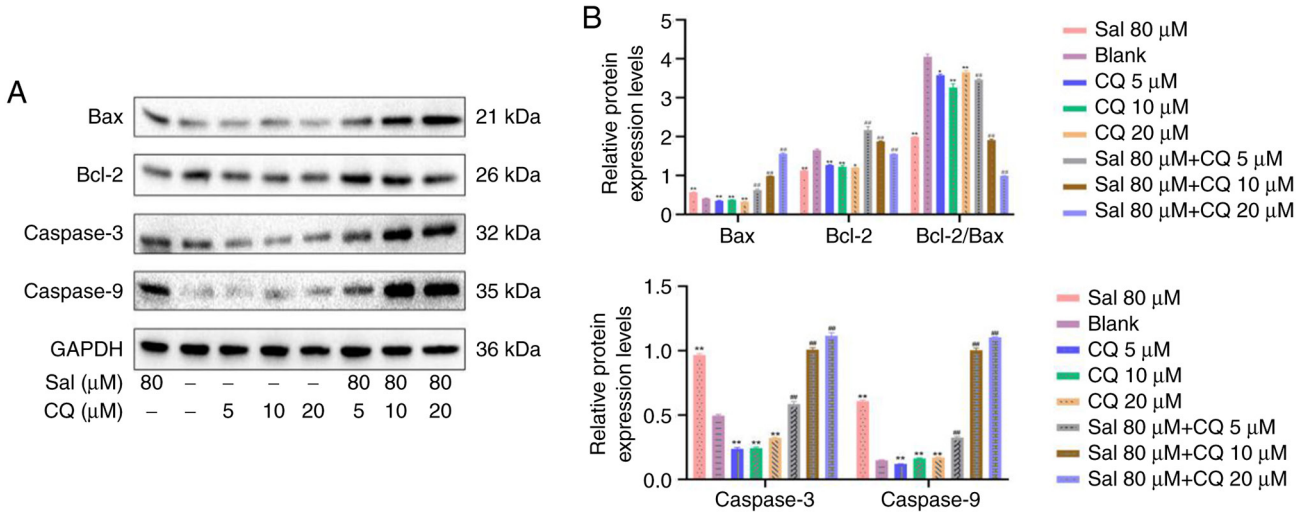

Figure 7. Inhibition of autophagy regulates expression levels of apoptosis-associated proteins in 97H cells. (A) Protein expression levels of Bax, Bcl-2, Caspase-3 and Caspase-9 were assessed using western blotting in 97H cells. (B) Protein expression levels of Bax, Bcl-2, Caspase-3 and Caspase-9 were semi-quantified using densitometry. **P<0.01 vs. blank. $^{\#\#}$P<0.01 vs. Sal. CQ, chloroquine diphosphate; Sal, salidroside.

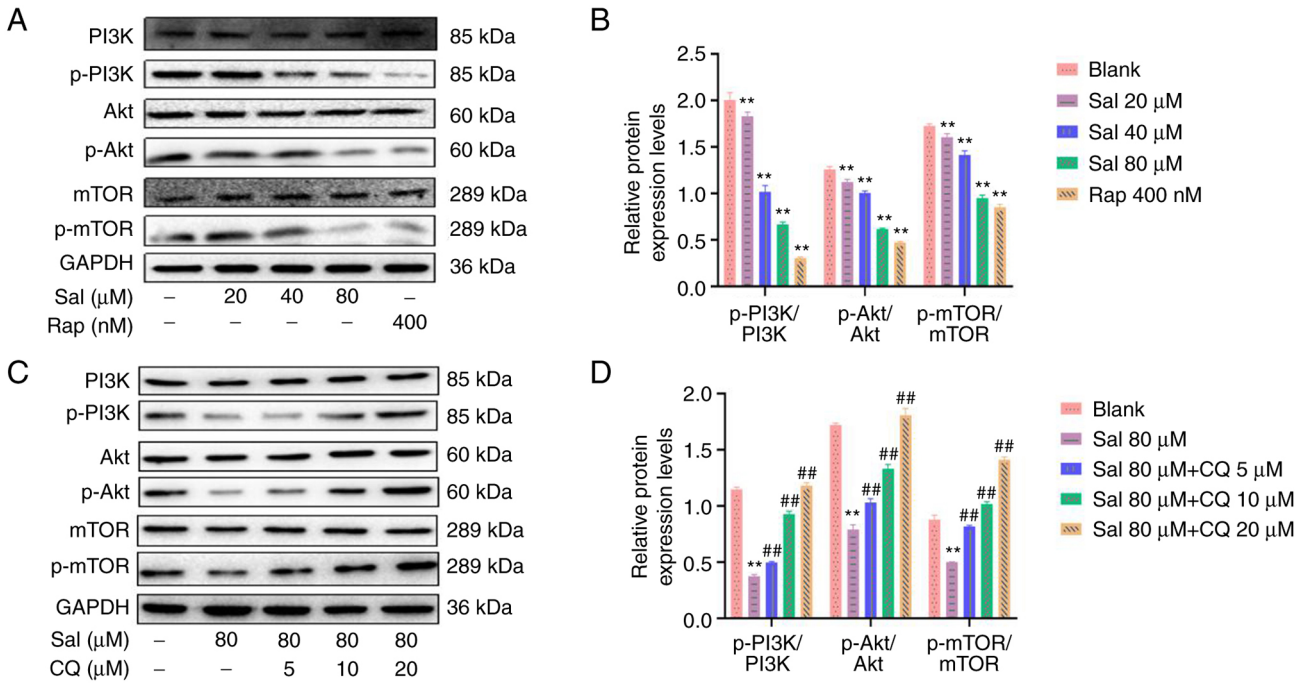

Figure 8. Expression levels of proteins associated with the PI3K/Akt/mTOR signaling pathway in 97H cells treated with Sal and CQ. (A) Expression levels of PI3K, p-PI3K, Akt, p-Akt, mTOR and p-mTOR proteins were assessed using western blotting in 97H cells treated with Sal or Rap. (B) Semi-quantification of PI3K, p-PI3K, Akt, p-Akt, mTOR and p-mTOR protein expression levels using densitometry. (C) Expression levels of PI3K, p-PI3K, Akt, p-Akt, mTOR and p-mTOR protein were assessed using western blotting in 97H cells treated with Sal and CQ. (D) Semi-quantification of PI3K, p-PI3K, Akt, p-Akt, mTOR and p-mTOR protein expression levels using densitometry. **P<0.01 vs. blank. $^{\#\#}$P<0.01 vs. Sal. CQ, chloroquine diphosphate; Sal, salidroside; Rap, rapamycin; p-, phosphorylated.

for autophagic evaluation and autophagy inhibitors were used as negative controls. CQ is a commonly used inhibitor of the autophagic pathway and has been reported to inhibit autophagy by prevention of the combination of autophagosomes and lysosomes (36). Furthermore, under normal conditions, autophagic flux of cells is low (59). If CQ is added first, autophagic flux could be too low to be detected. Therefore, 97H cells were pretreated with Sal and CQ was then used. CQ was used not only to evaluate autophagic induction of Sal in liver cancer cells, but also to evaluate the effect of the inhibition of autophagy on Sal-induced apoptosis of liver cancer cells. In the present study, in human 97H liver cancer cells, CQ and Sal in combination increased cell death markedly compared with Sal alone. This indicated that CQ enhanced Sal-induced liver cancer death and autophagy increased the apoptotic effect in 97H cells. Inhibitors of autophagy were used to evaluate the association between apoptosis and autophagy. Inhibition of Sal-induced autophagy promoting cell apoptosis; following

the inhibition of autophagy in Sal-treated cells, more apoptotic cells were observed.

The mitochondria, the energy metabolism center of cell, and serve an important role in the regulation of cell death and survival (60). Therefore, in the present study, TEM was used to evaluate the ultrastructure of mitochondria. The swollen mitochondria appeared in the Sal-treated group; however, following combination treatment with CQ, the morphological damage of mitochondria was more serious. The cascades triggered by the Caspase family serve a key role in the regulation of mitochondrial function (61). Caspase-3 has been reported to be downstream of this cascade reaction and causes cell death via degradation of intracellular substrates (62). Caspase-9, as a downstream signaling molecule of Caspase-3, damages the nuclear pore, which helps Caspase-3 enter the nucleus and hydrolyze deoxyribonuclease inhibitor (ICAD). ICAD is hydrolyzed and separated by Caspase-3 to release CAD, which causes DNA degradation, cytoskeleton separation and nuclear fragmentation, which leads to apoptosis (63). Therefore, the present study used western blotting to assess expression levels of Bax, Bcl-2, Caspase-3 and Caspase-9 proteins in Sal-treated 97H cells to evaluate the relationship between mitochondrial dysfunction and Caspase. Compared with Sal alone, using CQ and Sal in combination significantly increased protein expression levels of Caspase-3 and Caspase-9 and Bax/Bcl-2 ratio, which was associated with the damage to mitochondrial morphology. These results indicated that following treatment with Sal, inhibition of autophagy damaged the ultrastructure of cell mitochondria, which led to increased levels of cell apoptosis.

The PI3K/Akt signaling pathway is a classical pathway that regulates apoptosis. This signaling pathway affects the activity of downstream apoptosis-associated molecules (Bax, Bcl-2, Caspase-3 and Caspase-9) to regulate proliferation and apoptosis of cancer cells (64,65). For example, Chen and Liu (66) treated human gastric cancer SGC7901 cells with quercetin, which is extracted from Dendrobium bark, and reported that quercetin downregulated the protein expression levels of p-PI3K and p-Akt and upregulated the protein expression levels of Caspase-3, which indicated that quercetin induces apoptosis of SGC7901 cells via inhibition of the PI3K/Akt signaling pathway. Similarly, data from the present study demonstrated that Sal decreased phosphorylation of PI3K and Akt proteins and upregulated the protein expression levels of Bax/Bcl-2, Caspase-3 and Caspase-9. mTOR is not only a downstream target of the PI3K/Akt pathway but also serves an important role in the regulation of autophagy (67,68). For example, Rong *et al* (33) treated human gastric cancer AGS cells with Sal *in vitro* and reported that Sal treatment decreases protein expression levels of p-PI3K, p-Akt and p-mTOR and that combined treatment with Sal and autophagy inhibitor (insulin like growth factor-1, IGF-1) decreases expression levels of Beclin-1 and LC3-II proteins, which indicated that Sal induces autophagy in AGS cells via the PI3K/Akt/mTOR signaling pathway. Similarly, data from the present study demonstrated that Sal significantly decreased phosphorylation of PI3K, Akt and mTOR proteins, whereas combined treatment with Sal and CQ significantly increased expression levels of p-PI3K, p-Akt and p-mTOR proteins. Furthermore, Sal significantly upregulated the protein expression levels of Beclin-1 and LC3-II/LC3-I and significantly downregulated expression levels of p62 protein. These results suggested that Sal induced apoptosis and autophagy in human liver cancer cells via inhibition of the PI3K/Akt/mTOR signaling pathway.

In summary, the present study demonstrated that Sal induced 97H cell apoptosis via regulation of both mitochondrial function and the autophagic response. This may have involved the activation of both the PI3K/Akt/mTOR signaling pathway and directly or indirectly regulate mitochondrial dysfunction and autophagy for the survival of 97H cells. Following combination with autophagy inhibitor CQ, this autophagy was inhibited and Sal-induced apoptosis was increased. The present study demonstrated that autophagy may serve a role as a defense mechanism in Sal-treated human liver cancer cells and its inhibition may be a promising strategy for the adjuvant chemotherapy of liver cancer. However, the present study only evaluated the effects of one inhibitor in one cell line. Therefore, further research is required to evaluate the potential molecular mechanisms and develop targeted therapeutic drugs.

Acknowledgements

Not applicable.

Funding

This present study was supported by the Program of Technology Plan in Gansu Province (grant no. 18JR2FA010) and the Research Project of Traditional Chinese Medicine in Gansu Province (grant no. GZKP-2021-21).

Availability of data and materials

The datasets used and/or analyzed during the current study are available from the corresponding author on reasonable request.

Author's contributions

HS made substantial contributions to the conception and design of the present study. BJ performed the experiments. LF and TY acquired the data and confirm the authenticity of all the raw data. WG, YL and CL analyzed the data. BJ drafted the manuscript. HS and TW interpreted data and critically revised the manuscript. All authors have read and approved the final manuscript.

Ethics approval and consent to participate

Not applicable.

Patient consent for publication

Not applicable.

Competing interests

The authors declare that they have no competing interests.

References

1. Ferlay J, Colombet M, Soerjomataram L, Parkin DM, Piñeros M, Znaor A and Bray F: Cancer statistics for the year 2020: An overview. Int J Cancer: Apr 5, 2021 (Epub ahead of print).
2. Keda M, Morizane C, Ueno M, Okusaka T, Ishii H and Furuse J: Chemotherapy for hepatocellular carcinoma: Current status and future perspectives. Jpn J Clin Oncol 48: 103-114, 2018.
3. Kudo M: Targeted and immune therapies for hepatocellular carcinoma: Predictions for 2019 and beyond. World J Gastroenterol 25: 789-807, 2019.
4. Shin JW and Chung YH: Molecular targeted therapy for hepatocellular carcinoma: Current and future. World J Gastroenterol 19: 6144-6155, 2013.
5. Marin JJG, Briz O, Herraez E, Lozano E, Asensio M, Di Giacomo S, Romero MR, Osorio-Padilla LM, Santos-Llamas AI, Serrano MA, *et al*: Molecular bases of the poor response of liver cancer to chemotherapy. Clin Res Hepatol Gastroenterol 42: 182-192, 2018.
6. Qian KJ: Observation and prevention of side effects in interventional chemotherapy for liver cancer. J Clin Med Pract 4: 135-136, 2000.
7. Sun AH, Chen J and Guan HM: Reversal effect of paeonol on multidrug resistance of liver cancer cell line HepG2/ADM. Shandong Med J 56: 1-4, 2016.
8. Li W and Huang QN: Advances in studies and applications on *Rhodiola rosea* L. J Cap Norm Univ 3: 55-59, 2003.
9. Panossin A, Wikman G and Sarris J: Rosenroot (*Rhodiola rosea*): Traditional use, chemical composition, pharmacology and clinical efficacy. Phytomedicine 17: 481-493, 2010.
10. Booker A, Jalil B, Frommenwiler D, Reich E, Zhai L, Kulic Z and Heinrich M: The authenticity and quality of *Rhodiola rosea* products. Phytomedicine 23: 754-762, 2016.
11. Ruhsam M and Hollingsworth PM: Authentication of Eleutherococcus and Rhodiola herbal supplement products in the United Kingdom. J Pharm Biomed Anal 149: 403-409, 2018.
12. Ming DS, Hillhouse BJ, Guns ES, Eberding A, Xie S, Vimalanathan S and Towers GH: Bioactive compounds from *Rhodiola rosea* (crassulaceae). Phytother Res 19: 740-743, 2005.
13. Buchwald W, Mscisz A and Krajewska-Patan A: Contents of biologically active compounds in *Rhodiola rosea* roots during the vegetation period. Res Gate 10: 1413-1416, 2006.
14. Chen T, Ma Z, Zhu L, Jiang W, Wei T, Zhou R, Luo F, Zhang K, Fu Q, Ma C and Yan T: Suppressing receptor-interacting protein 140: A new sight for salidroside to treat cerebral ischemia. Mol Neurobiol 53: 6240-6250, 2016.
15. Shen JJ, Yuan LG and Li DD: Research on the anti-aging role of salidroside in naturally aged mice. Chin Med Bio 7: 412-417, 2012.
16. Wang S, He H, Chen L, Zhang W, Zhang X and Chen J: Protective effects of salidroside in the MPTP/MPP(+)-induced model of Parkinson's disease through ROS-NO-related mitochondrion pathway. Mol Neurobiol 51: 718-728, 2015.
17. Zheng T, Yang XY, Wu D, Xing S, Bian F, Li W, Chi J, Bai X, Wu G, Chen X, *et al*: Salidroside ameliorates insulin resistance through activation of a mitochondria-associated AMPK/PI3K/Akt/GSK3β pathway. Br J Pharmacol 172: 3284-3301, 2015.
18. Kerr JF, Wyllie AH and Currie AR: Apoptosis: A basic biological phenomenon with wide-ranging implications in tissue kinetics. Br J Cancer 26: 239-257, 1972.
19. Parzych KR and Klionsky DJ: An overview of autophagy: Morphology, mechanism, and regulation. Antioxid Redox Signal 20: 460-473, 2014.
20. Xiang YC, Peng P, Liu XW, Jin X, Shen J, Zhang T, Zhang L, Wan F, Ren YL, Yu QQ, *et al*: Paris saponin VII, a Hippo pathway activator, induces autophagy and exhibits therapeutic potential against human breast cancer cells. Acta Pharmacol Sin 43: 1568-1580, 2022.
21. Ji YC, Hu WW, Jin Y, Yu H and Fang J: Liquiritigenin exerts the anti-cancer role in oral cancer via inducing autophagy-related apoptosis through PI3K/AKT/mTOR pathway inhibition in vitro and in vivo. Bioengineered 12: 6070-6082, 2021.
22. Bata N and Cosford NDP: Cell survival and cell death at the intersection of autophagy and apoptosis: Implications for current and future cancer therapeutics. ACS Pharmacol Transl Sci 4: 1728-1746, 2021.
23. Wang Y, Liu CY and Wang ZY: Pseudolaric acid B induced autophagy through DNA damage response to inhibit apoptosis. Jilin J Chin Med 37: 381-384, 2017.
24. Shi Y, Han JJ, Tennakoon JB, Mehta FF, Merchant FA, Burns AR, Howe MK, McDonnell DP and Frigo DE: Androgens promote prostate cancer cell growth through induction of autophagy. Mol Endocrinol 27: 280-295, 2013.
25. Yang S, Wang X, Contino G, Liesa M, Sahin E, Ying H, Bause A, Li Y, Stommel JM, Dell'antonio G, *et al*: Pancreatic cancers require autophagy for tumor growth. Genes Dev 25: 717-729, 2011.
26. Zhang P, Sun Y and Yao YY: Effects of resveratrol on female reproductive system malignant tumors. J Dalian Med Univ 37: 403-407, 2015.
27. Zhan XJ, Xie DZ and Hu YY: Experimental study on anti-hepatocellular carcinoma and sensitizing effect of matrine combined with 5-fluorouracil in vitro. Jiangxi J Trad Chin Med 47: 42-45, 2016.
28. Chang MZ, Zhang SY and Hao YJ: Astragalus polysaccharide inhibits the proliferation of esophageal cancer EC109 cells by inducing cell autophagy. Central South Phar 20: 856-862, 2022.
29. Miao H, Yang JL, Zhang SQ and Yan N; Gynecology Third Treatment Area, Jilin Central Hospital: Effects of schisandra chinensis polysaccharides on proliferation, autophagy and endoplasmic reticulum stress apoptosis of ovarian cancer SKOV3 cells. Systems Med 6: 135-137, 2021.
30. Mai TT, Moon J, Song Y, Viet PQ, Phuc PV, Lee JM, Yi TH, Cho M and Cho SK: Ginsenoside F2 induces apoptosis accompanied by protective autophagy in breast cancer stem cells. Cancer Lett 321: 144-153, 2012.
31. Zhang Y, Bao J, Wang K, Jia X, Zhang C, Huang B, Chen M, Wan JB, Su H, Wang Y and He C: Pulsatilla saponin D inhibits autophagic flux and synergistically enhances the anticancer activity of chemotherapeutic agents against HeLa cells. Am J Chin Med 43: 1657-1670, 2015.
32. Wang J, Li JZ, Lu AX, Zhang KF and Li BJ: Anticancer effect of salidroside on A549 lung cancer cells through inhibition of oxidative stress and phospho-p38 expression. Oncol Lett 7: 1159-1164, 2014.
33. Rong L, Li Z, Leng X, Li H, Ma Y, Chen Y and Song F: Salidroside induces apoptosis and protective autophagy in human gastric cancer AGS cells through the PI3K/Akt/mTOR pathway. Biomed Pharmacother 122: 109726, 2020.
34. Jiang B, Yang T and Feng LF: Salidroside induces the autophagy of 97H cells. Gansu Med J 41: 193-197, 2022.
35. Lu L, Liu S, Dong Q and Xin Y: Salidroside suppresses the metastasis of hepatocellular carcinoma cells by inhibiting the activation of the Notch1 signaling pathway. Mol Med Rep 19: 4964-4972, 2019.
36. Pan WY, Zhu XD, Zhao W, Qu S, Li L, Su F and Li XY: The effects of chloroquine diphosphate and rapamycin at different concentration on autophagy of CNE-2 cells. Chin J Oncol Prev Treat 3: 280-283, 2011.
37. Zhang XY, Zhang YJ and Zhong Y: Research progress of mitochondrial dynamics disorder in cancer. Nat Rev Mol Cell Biol 28: 1219-1223, 2022.
38. DeVorkin L and Gorski SM: A mitochondrial-associated link between an effector caspase and autophagic flux. Autophagy 10: 1866-1867, 2014.
39. Kroemer G and Levine B: Autophagic cell death: The story of a misnomer. Nat Rev Mol Cell Biol 9: 1004-1010, 2008.
40. Mariño G, Niso-Santano M, Baehrecke EH and Kroemer G: Self-consumption: The interplay of autophagy and apoptosis. Nat Rev Mol Cell Biol 15: 81-94, 2014.
41. Fimia GM and Piacentini M: Regulation of autophagy in mammals and its interplay with apoptosis. Cell Mol Life Sci 67: 1581-1588, 2010.
42. Subramani R, Gonzalez E, Arumugam A, Nandy S, Gonzalez V, Medel J, Camacho F, Ortega A, Bonkoungou S, Narayan M, *et al*: Nimbolide inhibits pancreatic cancer growth and metastasis through ROS-mediated apoptosis and inhibition of epithelial-to-mesenchymal transition. Sci Rep 6: 19819, 2016.
43. Jiang PD, Zhao YL, Deng XQ, Mao YQ, Shi W, Tang QQ, Li ZG, Zheng YZ, Yang SY and Wei YQ: Antitumor and antimetastatic activities of chloroquine diphosphate in a murine model of breast cancer. Biomed Phaemacother 64: 609-614, 2010.
44. Sasaki K, Tsuno N, Sunami E, Tsurita G, Okaji Y, Nishikawa T, Syuno Y, Hongo K, Kitayama J, Takahashi K and Nagawa H: Abstract #383: Potentiation of pro-apoptotic effect of 5-fluorouracil on HT29 colon cancer cells by inhibition of autophagy. Cancer Res 69 (Suppl 9): S383, 2009.
45. Fan C, Wang W, Zhao B, Zhang S and Miao J: Chloroquine inhibits cell growth and induces cell death in A549 lung cancer cells. Bioorg Med Chem 14: 3218-3222, 2006.

46. Hao X and Li W: Chloroquine diphosphate suppresses liver cancer via inducing apoptosis in Wistar rats using interventional therapy. Oncol Lett 21: 233, 2021.
47. Zhou KJ, Wang C and Xie MY: Effect of chloroquine on tumor growth in mice with hepatic carcinoma and its mechanism. Anhui Med J 39: 1167-1170, 2018.
48. Wang ZB, Wang J and Wang L: Ultrastructural analysis of autophagosome. J Nanjing Med Uni (Nat Sci) 36: 426-429, 2016.
49. Zhang BN, Ye DY and Zhang DG: Application of laser confocal scanning microscope in observing autophagy. J Shantou Uni (Nat Sci Edi) 36: 76-81, 2021.
50. Cui QZ, Liu BY and Li YY: Hydroxysafflor yellow A represses Ang II-induced migration through activation of autophagy in VAFs. Chin Phar Bull 37: 1680-1687, 2021.
51. Wang YW and Hou JS: Function of autophagy gene Beclin 1 in tumor and its relationship with oral cancer. Chin J Pra Stom 4: 374-376, 2011.
52. Li BX, Li CY and Peng R: Expression of beclin-1, an autophagy-related protein, in stage IIIB colon cancer and its relationship with prognosis. Chin J Clin Onc 36: 146-149, 2009.
53. Zhang Q, Su H, Ranek MJ and Wang X: Autophagy and p62 in cardiac proteinopathy. Circ Res 109: 296-308, 2011.
54. Li XY, Zhao WD and Zhou Y: Expression of autophagy marker protein p62 in cervical squamous cell cancer and its clinical significance. Chin J Clin Exp Path 30: 38-41, 2014.
55. Kabeya Y, Mizushima N, Yamamoto A, Oshitani-Okamoto S, Ohsumi Y and Yoshimori T: LC3, GABARAP and GATE16 localize to autophagosomal membrane depending on form-II formation. J Cell Sci 117: 2805-2812, 2004.
56. Shen Y, Liang LZ, Hong MH, Xiong Y, Wei M and Zhu XF: Expression and clinical significance of microtubule-associated protein 1 light chain 3 (LC3) and Beclin1 in epithelial ovarian cancer. Ai Zheng 27: 595-599, 2008 (In Chinese).
57. Fan XJ, Wang Y, Wang L and Zhu M: Salidroside induces apoptosis and autophagy in human colorectal cancer cells through inhibition of PI3K/Akt/mTOR pathway. Oncol Rep 36: 3559-3567, 2016.
58. Ding SY, Wang MT, Dai DF, Peng JL and Wu WL: Salidroside induces apoptosis and triggers endoplasmic reticulum stress in human hepatocellular carcinoma. Biochem Biophys Res Commun 527: 1057-1063, 2020.
59. Esteban-Martínez L and Boya P: Autophagic flux determination in vivo and ex vivo. Methods 75: 79-86, 2015.
60. Zamzami N and Kroemer G: The mitochondrion in apoptosis: How Pandora's box opens? Nat Rev Mol Cell Biol 2: 67-71, 2001.
61. Chen AWG, Tseng YS, Lin CC, His YT, Lo YS, Chuang YC, Lin SH, Yu CY, Hsieh MJ and Chen MK: Norcantharidin induce apoptosis in human nasopharyngeal carcinoma through caspase and mitochondrial pathway. Environ Toxicol 33: 343-350, 2018.
62. Snigdha S, Smith ED, Prieto GA and Cotman CW: Caspase-3 activation as a bifurcation point between plasticity and cell death. Neurosci Bull 28: 14-24, 2012.
63. Fan TJ, Han LH, Cong RS and Liang J: Caspase family proteases and apoptosis. Acta Biochim Biophys Sin (Shanghai) 37: 719-727, 2005.
64. Noorolyai S, Shajari N, Baghbani E, Sadreddini S and Baradaran B: The relation between PI3K/AKT signalling pathway and cancer. Gene 698: 120-128, 2019.
65. Xu C, Sun G, Yuan G, Wang R and Sun X: Effects of platycodin D on proliferation, apoptosis and PI3K/Akt signal pathway of human glioma U251 cells. Molecules 19: 21411-21423, 2014.
66. Chen LY and Liu Y: Quercitrin promotes apoptosis of gastric cancer cell line SGC7901 by inhibiting PI3K/AKT signaling pathway. Chin J Pathophysiol 34: 1976-1980, 2018.
67. Fu WW, Ou YY and Huang CY: Research progress in the treatment of cardiovascular diseases based on mTOR regulating autophagy. J Hainan Med Univ 27: 635-640, 2021.
68. Kim KY, Park KI, Kim SH, Yu SN, Park SG, Kim YW, Seo YK, Ma JY and Ahn SC: Inhibition of autophagy promotes salinomycin-induced apoptosis via reactive oxygen species-mediated PI3K/AKT/mTOR and ERK/p38 MAPK-dependent signaling in human prostate cancer cells. Int J Mol Sci 18: 1088, 2017.